Journal of Statistical Physics, Vol. 57, Nos. 3/4, 1989

Properties of a Soft-Sphere Liquid from Non-Newtonian Molecular Dynamics

L. M. Hood,[1] D. J. Evans,[1] and H. J. M. Hanley[1,2]

Received March 10, 1989

A soft-sphere, inverse-12 liquid is simulated in both the isokinetic-isochoric and the isokinetic-isobaric ensemble using nonequilibrium molecular dynamics. The simulation for the isobaric ensemble is discussed in detail. The non-Newtonian characteristics of the liquid are clearly demonstrated; namely, the shear-rate-dependent pressure and density (shear dilatancy), the shear-rate-dependent shear viscosity (shear thinning), and evidence of normal pressure differences. For the first time, it is clearly shown that a significant component of isobaric shear thinning is due to shear dilatancy. The isochoric and isobaric results are checked for consistency. Simple empirical relations for the equation of state and transport properties of the fluid are presented.

KEY WORDS: Equation of state; isobaric ensemble; non-Newtonian molecular dynamics; rheology; soft-sphere liquid; transport coefficients.

1. INTRODUCTION

Non-Newtonian molecular dynamics has played a major role in recent studies of the physics of liquids.[1,2] The concept of the approach is simple[2–4]: since thermophysical properties of a system are insensitive to the details of the microscopic trajectories of the atoms or molecules in the thermodynamic limit, many sets of equations of motion can give identical and correct thermodynamic averages. Accordingly, we have the freedom to construct a simulation based on those equations of motion that are of the

[1] Research School of Chemistry, Australian National University, Canberra, ACT Australia, 2601.

[2] Permanent address: National Institute of Standards and Technology, Boulder, Colorado 80303.

0022-4715/89/1100-0729$06.00/0

most convenient for a particular problem. These equations will in general not be Newton's of the isolated microcanonical ensemble.

The power and versatility of non-Newtonian molecular dynamics are most obvious from the results obtained from nonequilibrium molecular dynamics (NEMD). Using NEMD, we and other authors have shown that a simple liquid is not simple at all when subjected to a shear and has rheological characteristics and behavior more often associated with fluids of complex structure. Examples are shear-rate-dependent viscosity coefficients and evidence of normal pressure differences in a sheared fluid.[2,5],[3]

The object of this paper is to present a precise self-consistent set of simulation data for the rheological and equilibrium properties of a typical simple liquid, and the soft sphere was selected as the model. A feature of the work is that we report consistent data from the isokinetic-isochoric *and* the isokinetic-isobaric ensemble.[7,8] We define isokinetic as the constant kinetic temperature constraint. The isobaric molecular dynamic simulations are new.

2. SIMULATION

We consider an N-particle inverse-12 soft-sphere liquid at a constant temperature T in volume V as a function of the soft-sphere state point x. The state point is defined by $x=\rho\sigma^3(\varepsilon/kT)^{1/4}$, where σ and ε are the usual potential parameters, and ρ is the density; $\rho=N/V$. The potential parameters, the mass m, and the temperature are set to unity; hence $x=\rho$. The simulation is set up to represent the liquid in stationary planar Couette flow subjected to a shear rate γ. The pressure p and shear viscosity η_+ are evaluated as a function of density and shear rate in the isokinetic-isochoric ensemble; and the density and shear viscosity are evaluated as a function of pressure and shear rate in the isokinetic-isobaric ensemble. We also evaluate viscosity coefficients that represent normal pressure differences in the fluid. As is the usual practice, all variables are dimensionless.

The operational definitions of the variables at a given density are as follows. The temperature,

$$3Nk_BT=\sum \mathbf{p}_i^2/m \tag{1}$$

where k_B is Boltzmann's constant and $\mathbf{p}_i$ is the peculiar momentum of particle i.

[3] See Ref. 6 which reports the proceedings of a conference on nonlinear phenomena held in Boulder, Colorado in 1982.

The pressure tensor **P**, defined by the equation

$$\mathbf{P}V = \sum \mathbf{p}_i \mathbf{p}_i / m + \sum \mathbf{q}_i \mathbf{F}_i \tag{2}$$

where $\mathbf{F}_i = \sum \partial \phi_{ij} / \partial \mathbf{r}_i$, with $\phi = 1/r^{12}$.

The hydrostatic pressure, given by

$$p(\gamma) = (1/3) \operatorname{tr} \mathbf{P} \tag{3}$$

The shear viscosity evaluated from the constitutive relation

$$P_{xy} = -\eta_+(\gamma)\gamma \tag{4}$$

with the strain rate defined as $\gamma = \partial u_x / \partial y$. Note that we allow the pressure and viscosity to be shear rate dependent.

Following Hess[9] and Hess and Hanley,[10] viscosity coefficients are defined to account for normal pressure differences

$$\eta_-(\gamma)\gamma = -(P_{xx} - P_{yy}) \tag{5}$$

and

$$\eta_0(\gamma)\gamma = -[P_{zz} - \tfrac{1}{2}(P_{xx} + P_{yy})] \tag{6}$$

2.1. Equations of Motion

The isobaric-isokinetic equations of motion for particle i in the system under shear can be written as

$$\dot{\mathbf{q}}_i = \frac{\mathbf{p}_i}{m} + \dot{\varepsilon}\mathbf{q}_i + \mathbf{i}\gamma q_{yi} \tag{7}$$

$$\dot{\mathbf{p}}_i = \mathbf{F}_i - \dot{\varepsilon}\mathbf{p}_i - \mathbf{i}\gamma p_{yi} - \alpha \mathbf{p}_i \tag{8}$$

where $\mathbf{i}$ is the unit vector in the x direction. The term α is a thermostatting multiplier which, for the Gaussian isokinetic equations of motion, is given by

$$\alpha = \frac{\sum \mathbf{F}_i \cdot \mathbf{p}_i - \gamma \sum p_{xi} \cdot p_{yi}}{\sum \mathbf{p}_i \cdot \mathbf{p}_i} \tag{9}$$

The dilation rate, $\dot{\varepsilon} = d\varepsilon/dt$, acts as a volume control to constrain the pressure and can be evaluated as follows. Consider the pressure in terms of Eq. (2),

$$3pV = \sum \mathbf{p}_i \cdot \mathbf{p}_i / m + \sum \mathbf{q}_i \cdot \mathbf{F}_i$$

$$= \sum \mathbf{p}_i \cdot \mathbf{p}_i / m - \frac{1}{2} \sum_{i \neq j} \mathbf{q}_{ij} \cdot \mathbf{F}_{ij} \tag{10}$$

The time derivative of this equation is

$$3p\dot{V}+3\dot{p}V=\sum 2\mathbf{p}_i\cdot\frac{\dot{\mathbf{p}}_i}{m}-\frac{1}{2}\sum_{i\neq j}\left[\dot{\mathbf{q}}_{ij}\cdot\mathbf{F}_{ij}+\mathbf{q}_{ij}\cdot\left(\frac{\partial\mathbf{F}_{ij}}{\partial\mathbf{q}_{ij}}\cdot\dot{\mathbf{q}}_{ij}\right)\right] \tag{11}$$

However, the second term on the left-hand side is zero at constant pressure, and the first term on the right-hand side is zero at constant temperature. For the spherically symmetric potential ϕ,

$$\begin{aligned}3p\dot{V}&=-\frac{1}{2}\sum_{i\neq j}\left[\dot{\mathbf{q}}_{ij}\cdot\mathbf{F}_{ij}+\mathbf{q}_{ij}\cdot\left(\frac{\partial^2\phi_{ij}}{\partial\mathbf{q}_i^2}\cdot\dot{\mathbf{q}}_{ij}\right)\cdot\dot{\mathbf{q}}_{ij}\right]\\&=-\frac{1}{2}\sum_{i\neq j}\left\{\dot{\mathbf{q}}_{ij}\cdot\mathbf{F}_{ij}+\mathbf{q}_{ij}\cdot\left[\frac{\phi'_{ij}}{\mathbf{q}_{ij}}\mathbf{I}-\frac{\mathbf{q}_{ij}\mathbf{q}_{ij}}{\mathbf{q}_{ij}^2}\left(\frac{\phi'_{ij}}{\mathbf{q}_{ij}}-\phi''_{ij}\right)\right]\cdot\dot{\mathbf{q}}_{ij}\right\}\end{aligned} \tag{12}$$

which reduces to

$$3p\dot{V}=-\frac{1}{2}\sum_{i\neq j}\left[\dot{\mathbf{q}}_{ij}\cdot\mathbf{F}_{ij}+\phi''_{ij}(\mathbf{q}_{ij}\cdot\dot{\mathbf{q}}_{ij})\right] \tag{13}$$

On substitution into the equations of motion with the relation

$$\dot{V}=3\dot{\varepsilon}V \tag{14}$$

and the definition

$$\Phi_{ij}\equiv\frac{\phi'_{ij}}{\mathbf{q}_{ij}}+\phi''_{ij} \tag{15}$$

we get the expression

$$\dot{\varepsilon}=\left[-\frac{1}{2}\sum_{i\neq j}\Phi_{ij}\left(\frac{\mathbf{q}_{ij}\cdot\mathbf{p}_{ij}}{m}+\gamma q_{ijx}q_{ijy}\right)\right]\Big/\left(\frac{1}{2}\sum_{i\neq j}\Phi_{ij}\,\mathbf{q}_{ij}^2+9pV\right) \tag{16}$$

The pressure constraint sets the time derivative of the pressure to zero, rather than constraining the pressure itself to a particular value. Thus, to simulate the system at a given pressure, we introduce the Newton–Raphson procedure to alter the volume until the pressure is constant at the desired value to within specified limits. Further, the pressure and temperature drift slowly with time because of numerical inaccuracies. Hence, we have to to rescale occasionally, typically every 25–100 timesteps, before the drift has become appreciable. The pressure is rescaled using the Newton–Raphson technique, while the temperature is rescaled using simple velocity rescaling.

The difficulties can be avoided with a Nosé–Hoover feedback procedure.[11,12] The time derivative of a feedback variable is related to the

difference between the value of the variable at a given time step and the desired or targeted value. The feedback variable is the pressure for an isobaric simulation, and the time derivative is proportional to the dilation rate. We write

$$\ddot{\varepsilon} = \frac{1}{Q_p}(p - p_{\text{target}}) \tag{17}$$

where Q_p is a damping constant. Note that this constraint does not fix the pressure, but constrains it to fluctuate about the desired value. There is no prescription for choosing a value for the damping constant but, fortunately, we have found that the average values of the properties of the system are only weakly dependent on it.[13] Based on trial and error, we fix Q_p at 10. It was found in practice that there was no significant difference in the simulation results if either Eq. (16) or (17) was used to constrain the pressure.

2.2. Procedure

The system studied consisted of 256 soft spheres interacting with an inverse-12 potential truncated at $r_c = 1.5\sigma$. Runs were carried out with a reduced timestep $\Delta t = 0.004$ for the smaller shear rates ($\gamma \leqslant 1.0$) and $\Delta t = 0.002$ otherwise. The runs varied in length from 2 million timesteps for the larger shear rates to 25 million timesteps for the smallest shear rate studied, $\gamma = 0.0625$. The calculations were performed using a neighbor list algorithm similar to the one described by Fincham and Ralston[14] with complete vectorization of the forces loop, including the force summation.

Calculations were carried out at state points in the range $0.8485 < \rho < 1.0607$, where the freezing density of the 256-particle system is 1.15, and for the equivalent reduced pressures, $8.143 < p < 17.0$. Data were taken for the system in equilibrium ($\gamma = 0$), and when subjected to a shear in the range $0.64 < \gamma < 1.55$. The shear-rate range was extended at the density of 0.9899 since this particular state point corresponded to that selected in our previous work.[7,10]

3. RESULTS

3.1. Pressure-Density

Figure 1 shows a plot of the pressure as a function of shear rate at constant density. One observes the $\gamma^{3/2}$ dependence as reported in earlier work.[5,10] Figure 2 shows the corresponding curves in the isobaric ensem-

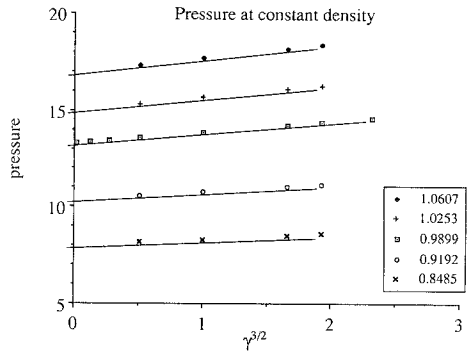

Fig. 1. Plot of the pressure p and shear rate for the dense, soft-sphere liquid at several densities. The freezing density is 1.15. The pressure varies as $\gamma^{3/2}$.

ble: again the $\gamma^{3/2}$ dependence is clear. We estimate the data to be precise to 0.01 %.

The equilibrium data were compared with the data, taken over a wide range of state points reported by Hoover *et al.*[15,16], and other authors,[10] summarized in ref. 17.[4] A sample comparison for the equilibrium compressibility factor is given in Fig. 3. The new results are lower, although well within the estimated precision of all data sets.

The results here were fitted to simple polynomials consistent with the smoothing equations in ref. 17,

$$p_{eq} = \rho T * (1.0 + 3.31769 * \rho - 0.685244 * \rho^2 + 10.131153 * \rho^3) \quad (18)$$

$$p_\gamma = \rho T * (0.092405 * \rho + 0.074186 * \rho^2 + 0.432951 * \rho^3) \quad (19)$$

$$p = p_{eq} + p_\gamma * \gamma^{3/2} \quad (20)$$

[4] See ref. 17, Eqs. (44)–(47). Note the misprint in Eq. (45): for 0.2982 read 0.02982.

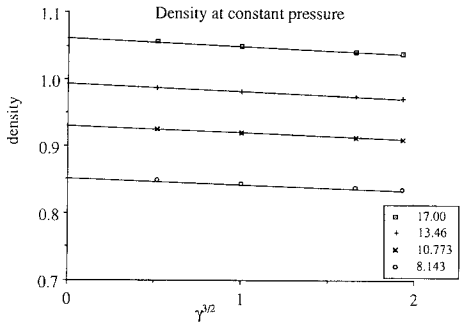

Fig. 2. Plot corresponding to Fig. 1 showing the variation of density with $\gamma^{3/2}$ at constant pressure.

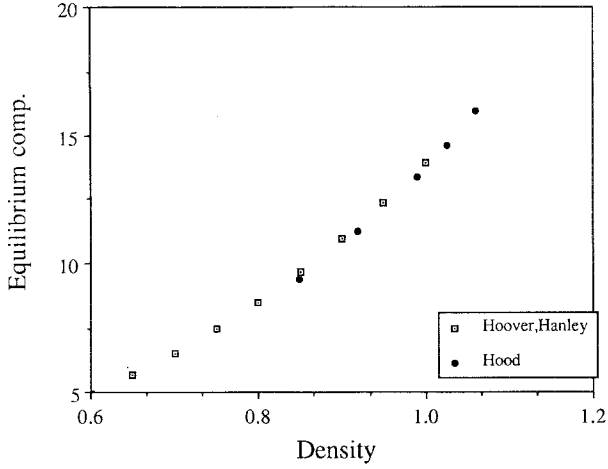

Fig. 3. Comparison of the equilibrium compressibility factor at high densities. The data are compared with those from previous work of Hoover and of Hanley represented by the smoothing equation in ref. 17.

Expressions for the density as a function of pressure are given in the Appendix. Note that Eqs. (18) and (19), and the equations in the Appendix, are merely fitting functions; they extrapolate correctly to zero density, but are not exact for the moderately dense gas. A detailed discussion on the second and third virial coefficients of the soft-sphere gas is given by Rainwater.[18]

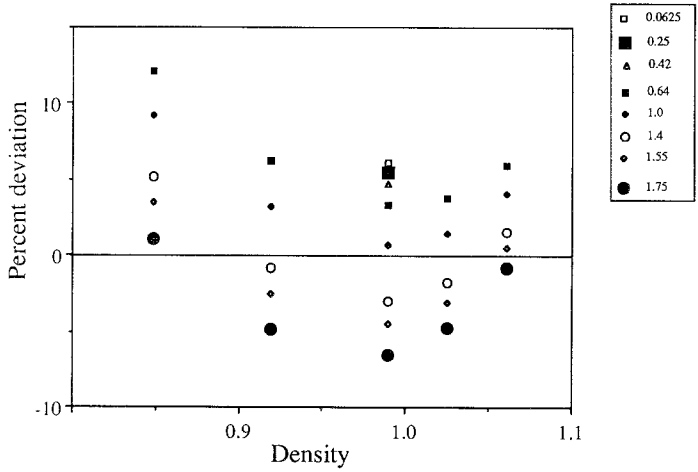

Fig. 4. Evaluation of Eq. (21) at various shear rates Percent deviation is defined as (lhs − rhs) * 100/lhs.

Since the pressure is a function of density and shear rate, we have

$$(\partial p/\partial \gamma)_{\rho,T} = -(\partial p/\partial \rho)_{\gamma,T}\,(\partial \rho/\partial \gamma)_{p,T} \tag{21}$$

This relation was checked and the result shown graphically as Fig. 4. There is some systematic error; the bow deviation pattern as a function of density is due to large uncertainties in the derivative $(\partial \rho/\partial \gamma)_{p,T}$ that is close to zero. The spread at constant density is due to errors in $(\partial p/\partial \rho)_{\gamma,T}$. Nevertheless, the check is considered satisfactory based on our experience in fitting experimental equation-of-state and thermodynamic data, and does not warrant adjusting the simple functions forms or the coefficients of Eqs. (18)–(20).

3.2. Shear Viscosity

Figures 5 and 6 show the variation of the shear viscosity with shear rate at constant density and pressure, respectively. We have assumed a $\gamma^{1/2}$ dependence as in most previous studies, although the constant-density plot, in particular, is not entirely consistent with this assumption over all γ. In view of the errors in the data, assessed as 0.5%, and a consistency check from the expression

$$(\partial \eta_+/\partial \gamma)_{p,T} = (\partial \eta_+/\partial \rho)_{\gamma,T}\,(\partial \rho/\partial \gamma)_{p,T} + (\partial \eta_+/\partial \gamma)_{\rho,T} \tag{22}$$

the $\gamma^{1/2}$ dependence is justified. Equation (22) is satisfied to within 12% or better.

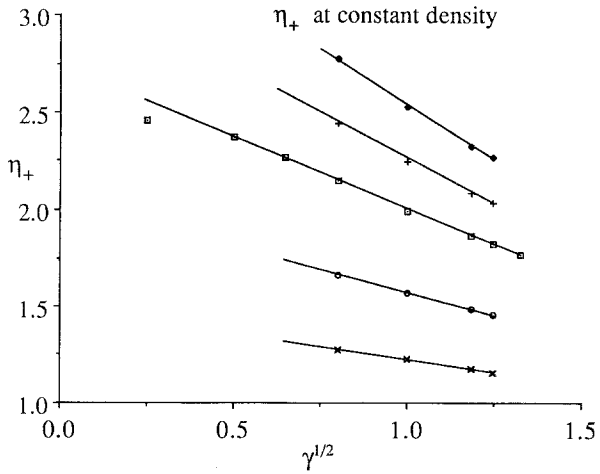

Fig. 5. Variation of the shear viscosity η_+ with $\gamma^{1/2}$ at constant density. Legend as in Fig. 1.

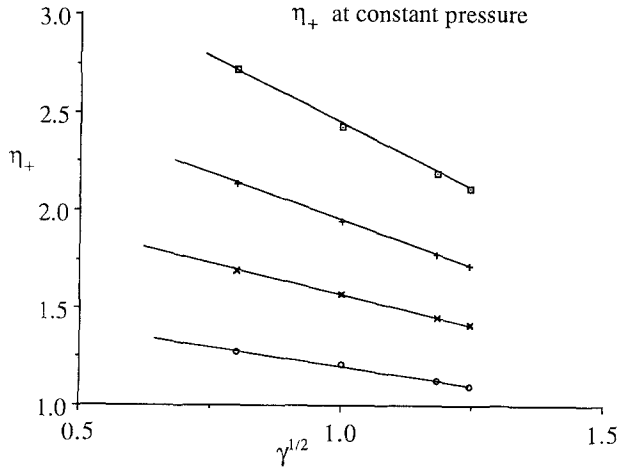

Fig. 6. Variation of the shear viscosity with $\gamma^{1/2}$ at constant pressure. Legend as in Fig. 2.

The isochoric data were compared to previous results of Ashhurst and Hoover,[19] Hess and Hanley,[10] and other authors.[6] The Newtonian viscosity at zero γ agreed well, but the $\gamma^{1/2}$ dependence of our data was slightly weaker than that observed previously. Using data from the smoothing equations in ref. 17 to ensure a well-behaved function at the lower densities, one finds the zero-γ viscosity to be represented by the expression

$$\eta^+_{\gamma=0} = 0.171 + 0.025604 * [\exp(46.579 * \rho) - 1.0] \tag{23}$$

Equation (23) is proposed only to give a fit of the data. It does not give the correct moderately dense behavior, for example.[20] The shear-rate dependence is represented by simple equations given in the Appendix.

3.3. Normal Pressure Differences

The coefficients defined by Eqs. (5) and (6) are displayed as Figs. 7–10. They are well-behaved functions of the shear rate, but the low-γ behavior is uncertain. We have found repeatable negative values at low γ for the 256-particle system (and for the 56- and 108-particle liquids), but it is unclear if corresponding negative values would be found for a larger system. Excluding these points, we estimate the uncertainty in the coefficients to be 6 and 3% for η_- and η_0, respectively. Our expressions for the coefficients are given in the Appendix. It is seen that η_- is a very weak function of the shear rate, excluding the low-γ points. For this reason, a consistency check

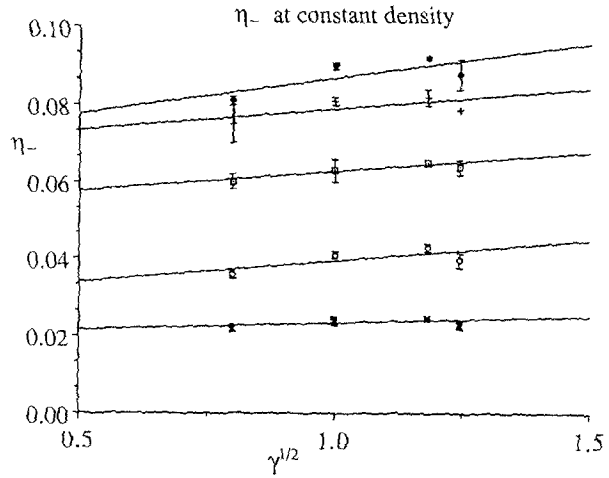

Fig. 7. Variation of the normal pressure difference coefficient η_- with $\gamma^{1/2}$ at constant density. Legend as in Fig. 1. Negative values at the low γ are not shown. It is not clear if these negative points are realistic.

from the expression equivalent to Eq. (22) is not reasonable, but the corresponding check for the coefficient η_0 is within 15%, a very satisfactory result.

4. DISCUSSION AND CONCLUSION

We have discussed the quantiative behavior of the pressure, the density, and the viscosity coefficients of the soft-sphere model liquid when sub-

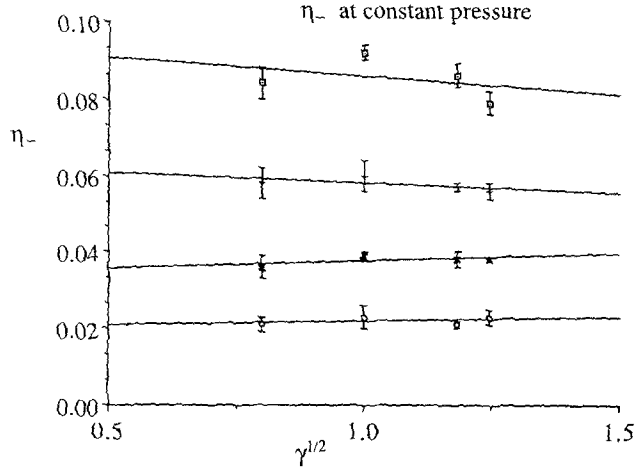

Fig. 8. Variation of η_- with $\gamma^{1/2}$ at constant pressure. Legend as in Fig. 2.

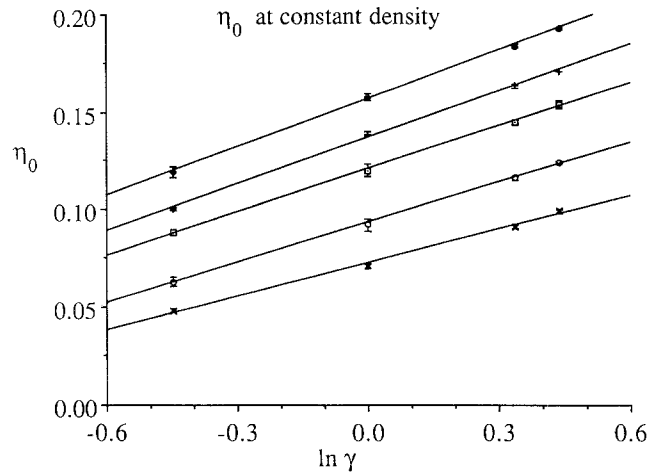

Fig. 9. Variation of the normal pressure difference coefficient η_0 with $\ln \gamma$ at constant density. Legend as in Fig. 1. Negative values at the low γ are not shown.

jected to a shear. Results have been presented graphically and represented by simple empirical equations. A feature of this work was that simulations were carried out in the isochoric and the isobaric ensembles and we have demonstrated that the data are self-consistent. For the first time we have a quantitative estimate of the pressure and density dependence of the coefficients that represent normal pressure differences.

Having data in both the isochoric and the isobaric ensemble allows one to check a point that has caused much confusion in the rheology

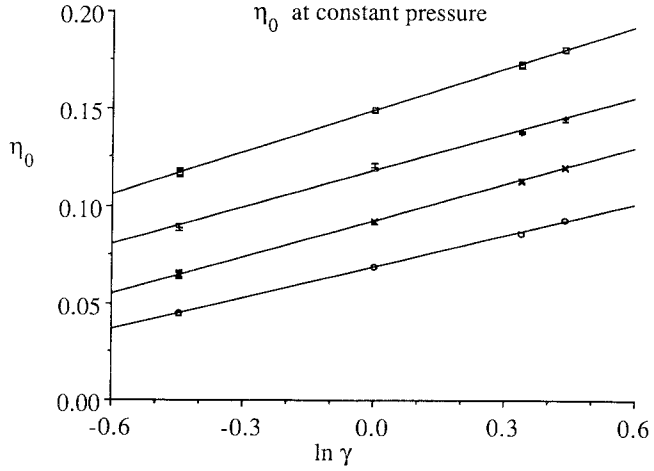

Fig. 10. Variation of η_0 with $\ln \gamma$ at constant pressure. Legend as in Fig. 2.

literature; namely, the difference between shear thinning, the reduction in viscosity with increasing shear rate, and shear dilatancy, the increase in volume with increasing shear rate at constant pressure. Figure 11 shows the viscosity as a function of shear rate for our system at constant pressure and at constant density. The important feature to note from this graph is that a *significant* component of the isobaric shear thinning is due to the shear dilatancy. This is clear from Eq. (22), but is the first time that such a result has been unequivocally demonstrated.

Since the potential contribution to the energy of an inverse-12 soft sphere is trivially related to the potential part of the pressure by $E = 4\rho$, sufficient information has been given for a comprehensive picture of the thermodynamic properties of the fluid. There are now several parallel studies of the structure and behavior of inverse-power model fluids in terms of simulations of the radial distribution function and the structure factor.[17,21,22] Overall, therefore, we have a very complete description of the shear-induced behavior of a simple liquid.

Finally, we remark that numerical thermophysical property information is essential if any physical problem is to be understood. Of relevance here, for example, the statistical mechanical mechanics and thermodynamics of a nonequilibrium system have been a topic of interest[4] for some time, but progress and understanding has been slow because many results were only formal and could not be verified until recently.[23] Also, as Rainwater *et al.*[17] have pointed out, if the shear-rate-dependent properties of a system are known *a priori*, one can approach fluid dynamics and

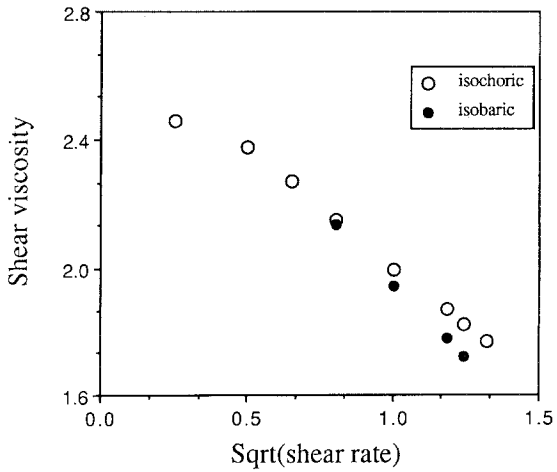

Fig. 11. Variation of the shear viscosity with $\gamma^{1/2}$ at constant pressure and at constant density. The graph illustrates that a significant component of shear thinning is due to shear dilatancy.

rheology directly. Traditionally, fluid dynamics is approached by describing the motion of the fluid in macroscopic terms and inferring the properties of the fluid after making specific assumptions such as the neglect of compressibility.

APPENDIX

This Appendix contains simple fitting equations of the soft-sphere properties obtained from the simulation. The equations are empirical. All variables are in reduced units with the reducing parameters set equal to one.

Density–pressure with $p > 8.143$ and $0.64 < \gamma < 1.55$:

$$\begin{aligned} \rho_{eq} &= 0.54561 + 0.44763e\text{-}1 * p - 0.84681e\text{-}3 * p^2 \\ \rho_\gamma &= 0.1309e\text{-}2 + 0.13413e\text{-}2 * p - 0.399e\text{-}4 * p^2 \\ \rho &= \rho_{eq} - \rho_\gamma * \gamma^{3/2} \end{aligned} \tag{A1}$$

Shear viscosity–density, with $\rho > 0.8485$ and $0.64 < \gamma < 1.55$:

$$\begin{aligned} \eta_0^+ &= 0.11738e{+}2 - 0.70755e{+}1 * \gamma^{1/2} \\ \eta_1^+ &= -0.29903e{+}2 + 0.17672e{+}2 * \gamma^{1/2} \\ \eta_2^+ &= 0.2103e{+}2 - 0.11390e{+}2 * \gamma^{1/2} \\ \eta_+ &= \eta_0^+ + \eta_1^+ * \rho + \eta_2^+ * \rho^2 \end{aligned} \tag{A2}$$

Shear viscosity–pressure, with $p > 8.143$ and $0.64 < \gamma < 1.55$:

$$\begin{aligned} \eta p_0^+ &= -0.46187 + 0.51493 * \gamma^{1/2} \\ \eta p_1^+ &= 0.25067 - 0.11014 * \gamma^{1/2} \\ \eta_+ &= \eta p_0^+ + \eta p_1^+ * p \end{aligned} \tag{A3}$$

Viscosity η_0 and density, with $\rho > 0.8485$ and $0.64 < \gamma < 1.55$:

$$\begin{aligned} \eta_1^0 &= 0.40169 - 0.10138e + 1 * \rho + 0.73771 * \rho^2 \\ \eta_2^0 &= -0.3943e\text{-}1 + 0.11376 * \rho \\ \eta_0 &= \eta_1^0 + \eta_2^0 * \ln \gamma \end{aligned} \tag{A4}$$

Viscosity η_0 and pressure, with $p > 8.143$ and $0.64 < \gamma < 1.55$:

$$\begin{aligned} \eta p_0^0 &= -0.5152e\text{-}2 + 0.90903e\text{-}2 * p \\ \eta p_1^0 &= 0.3869e\text{-}1 + 0.19342e\text{-}2 * p \\ \eta_0 &= \eta p_0^0 + \eta p_1^0 * \ln \gamma \end{aligned} \tag{A5}$$

Viscosity η_- and density, with $\rho > 0.8485$ and $0.64 < \gamma < 1.55$:

$$\begin{aligned} \eta_0^- &= 0.56677e\text{-}1 + 0.32402e\text{-}1 * \gamma^{1/2} \\ \eta_1^- &= -0.28629 - 0.10419 * \gamma^{1/2} \\ \eta_2^- &= 0.28446 + 0.83314e\text{-}1 * \gamma^{1/2} \\ \eta_- &= \eta_0^- + \eta_1^- * \rho + \eta_2^- * \rho^2 \end{aligned} \tag{A6}$$

Viscosity η_- and pressure, with $p > 8.143$ and $0.64 < \gamma < 1.55$:

$$\begin{aligned} \eta p_0^- &= -0.556e\text{-}1 + 0.16509e\text{-}1 * \gamma^{1/2} \\ \eta p_1^- &= 0.82843e\text{-}2 - 0.94301e\text{-}3 * \gamma^{1/2} \\ \eta_- &= \eta p_0^- + \eta p_1^- * p \end{aligned} \tag{A7}$$

ACKNOWLEDGMENTS

Part of this work was sponsored by the Department of Energy, Office of Basic Energy Sciences. H. Hanley is very grateful to the faculty and staff of the RSC, Australian National University, for their hospitality. The calculations were performed at the ANU Supercomputer Facility.

REFERENCES

1. D. J. Evans and W. G. Hoover, *Annu. Rev. Fluid Mech.* **18**:243 (1986).
2. H. J. M. Hanley and D. J. Evans, *Int. J. Thermophys.*, in press (1988).
3. D. J. Evans and G. P. Morriss, *Comp. Phys. Rep.* **1**:299 (1984).
4. D. J. Evans and G. P. Morriss, *Dynamics of Classical Liquids* (Academic Press, New York, in press).
5. D. J. Evans, H. J. M. Hanley, and S. Hess, *Phys. Today* **3**:26 (1984).
6. *Physica* **118a** (1983).
7. D. J. Evans and G. P. Morriss, *Chem. Phys.* **7**:63 (1983).
8. H. J. M. Hanley, J. C. Rainwater, D. J. Evans, and L. M. Hood, in *Proceedings Xth International Congress of Rheology*, P. H. T. Uhlherr, ed. (Sydney, 1988).
9. S. Hess, *Phys. Rev. A* **25**:614 (1982).
10. S. Hess and H. J. M. Hanley, *Int. J. Thermophys.* **4**:97 (1983).
11. S. Nosé, *Mol. Phys.* **52**:255 (1984).
12. W. G. Hoover, *Phys. Rev. A* **31**:1695 (1985).

13. L. M. Hood, D. J. Evans, and G. P. Morriss, *Mol. Phys.* **62**:419 (1987).
14. D. Fincham and B. J. Ralston, *Comput. Phys. Comm.* **23**:127 (1981).
15. W. G. Hoover, M. Ross, K. W. Johnson, D. Henderson, J. A. Barker, and B. C. Brown, *J. Chem. Phys.* **52**:4931 (1970).
16. F. J. Rogers and D. A. Young, *Phys. Rev. A* **30**:999 (1984).
17. J. C. Rainwater, H. J. M. Hanley, T. Paszkiewicz, and Z. Petru, *J. Chem. Phys.* **83**:339 (1985).
18. J. C. Rainwater, *J. Stat. Phys.* **19**:177 (1978).
19. W. T. Ashhurst and W. G. Hoover, *Phys. Rev. A* **11**:658 (1975).
20. J. C. Rainwater, *J. Chem. Phys.* **71**:5171 (1979); **74**:4130 (1981).
21. H. J. M. Hanley, G. P. Morriss, T. R. Welberry, and D. J. Evans, *Physica* **149a**:406 (1988).
22. H. J. M. Hanley, J. C. Rainwater, and S. Hess, *Phys. Rev. A* **36**:1795 (1987).
23. D. J. Evans and E. G. D. Cohen, *J. Stat. Phys.*, this issue (1989).